JOURNAL OF AGRICULTURAL AND FOOD CHEMISTRY

# Monitoring of Moisture Redistribution in Multicomponent Food Systems by Use of Magnetic Resonance Imaging

PEDRO RAMOS-CABRER,[†,‡] JOHN P. M. VAN DUYNHOVEN,*[,§] HANS TIMMER,[§] AND KLAAS NICOLAY[⊥]

Department of Experimental in vivo NMR, Image Sciences Institute (ISI), University Medical Centre, Bolognalaan 30, 3583 CJ Utrecht, The Netherlands, Unilever Food and Health Research Institute (UFHRI), Olivier van Noortlaan 120, 3133 AT Vlaardingen, The Netherlands, and Department of Biomedical Engineering (BME), Eindhoven University of Technology, P.O. Box 513, 5600 MB Eindhoven, The Netherlands

Differences in water activity within multicomponent food systems inevitably lead to moisture (re)-distribution phenomena, hence deteriorating textural quality during shelf life. Noninvasive assessment of moisture transport in such systems would promote mechanistic understanding and enable rational development of strategies to control migration. Magnetic resonance imaging (MRI) is an ideal candidate for such a measurement technique, but its use in systems with low-moisture components (e.g., cereal materials) is seriously hampered because of reduced transverse relaxation times. In this work, we report two MRI protocols for the noninvasive and quantitative assessment of moisture transport in multicomponent food products. The first protocol is suitable to study relatively slow (days/weeks) processes, whereas the second one is designed to study fast (hours) moisture transport. We have successfully applied this methodology to quantify moisture transport within multicomponent food systems, with adequate temporal and spatial resolution.

**KEYWORDS: MRI; single-point imaging; SPI; moisture transport; low-moisture; water; snacks**

## INTRODUCTION

Nowadays, food products are increasingly consumed 'on the go' in out of home channels. As a consequence, the consumer's demand for ready to eat food products, such as snacks, has been largely increased in the past decades. In most of these products, consumer appreciation is mainly provided by contrast in texture between different components of the product. With the current technology, this implies contrast in water activity (Aw) and hence a nonequilibrium thermodynamic state. Without proper precautions, this inevitably leads to moisture migration, with subsequent loss in textural quality during shelf life of the product (*1*). Therefore, a major challenge in the development of multicomponent food products, with ambient stable texture contrast, is to design strategies to control moisture migration (*2*). When the effect of such strategies can be assessed in a noninvasive manner, this can aid significantly in the development of novel multicomponent food (snack) products. Furthermore, noninvasive assessment of moisture migration in multicomponent food products can also yield valuable data for development and validation of transport models. Currently, such models are based on either indirect (*3*, *4*) or invasive procedures (*5*).

One of the most outstanding noninvasive techniques available to study water status in solidlike materials is magnetic resonance imaging (MRI). Contrast in MRI images is governed by the local physicochemical properties of the system. The ability of MRI to provide spatially resolved information noninvasively, and without the use of ionizing radiation, is especially attractive for the study of multicomponent food systems. However, the conventional MRI techniques are typically designed for component with high molecular mobility, where the transverse relaxation times (T2) are rather long (>ms). This regime is particularly suited for medical applications, where conventional MRI methods are able to provide detailed descriptions of mobility populations (e.g., *6*). However, such techniques are insensitive to molecules with low mobility, for which the transverse relaxation times are very short (< ms) (*7*). In this regime, transverse relaxation times are denoted as T2*.

The limitations of conventional MRI have hampered its application to a major class of food systems, i.e., where mobility of water is restricted because of its strong association with the matrix. Hence, recourse was taken to nonconventional solid-state MRI techniques, commonly denoted as single-point imaging (SPI) (*8*). Using SPI techniques, it is possible to obtain images from systems with T2* values as short as a few tens of

* To whom correspondence should be addressed. E-mail: John-van.duynhoven@ unilever.com. Phone: +31 10 4605534. Fax: +31 10 4605310.
[†] ISI, Utrecht.
[§] UFHRI, Vlaardingen.
[⊥] BME, Eindhoven.
[‡] Present address: In-vivo-NMR Laboratory, Max-Planck-Institute for Neurological Research, Gleuelerstrasse 40, D-50931 Koln, Germany.

10.1021/jf052246z CCC: $33.50 
Published on Web 01/13/2006

microseconds using conventional scanners, although with limited spatial and temporal resolution (*9*).

The different time scales of moisture transport require protocols where different compromises are made with respect to scanning time and the resolution of mobility regimes. Within applications of MRI, there is always a tradeoff between (1) sensitivity, (2) spatial resolution, (3) temporal resolution, and (4) the range of molecular mobility regimes that can be studied. When one of these requirements is favored, this will always be at the expense of at least one of the other three. Hence, to yield valuable information, the development of an experimental MRI protocol involves a careful balance of these four requirements. This is particularly challenging when MRI is applied to study multicomponent food products since this often involves the observation of components with high and low molecular mobilities. This stands in contrast to most biomedical MRI applications, which tend to be blind to low molecular mobility components. Furthermore, components with low molecular mobility, such as bread, also have a low proton density, hence requiring maximal sensitivity. Currently, the SPI methods have most room to maneuver with spatial and temporal resolution for low mobility systems. Although SPI has previously been applied to food systems (*10*, *11*), the resulting images were treated in a qualitative manner.

The shortcomings of the MRI approaches described so far have prompted us to investigate whether SPI can be deployed to quantitatively monitor moisture migration in food systems where at least one of the components has a low molecular mobility. For this purpose, we introduced two experimental protocols to obtain quantitative information on moisture transport: protocol 1 to study slow processes and protocol 2 for (relative) fast ones. The protocols were applied to systems where bread was combined with soft and moist components. The difference in water activity between these components resulted in migration rates that ranged from weeks (protocol 1) to days (protocol 2).

## MATERIALS AND METHODS

**MR Image Acquisition and Processing.** MR images were acquired using a 4.7 T horizontal bore magnet (Oxford Instruments, Abingdon, U.K.), operated with a Varian INOVA console (Varian, Palo Alto, CA), and equipped with an auto-shielded gradient insert (450 mT/m) of 12 cm internal diameter (Magnex Scientific, Oxford, U.K.). Two different birdcage coils, with an effective length of 10 cm and diameters of 6.4 and 8.9 cm, were used for both signal transmission and detection.

Fractions of water molecules with high mobility (long T2 values) were imaged using a conventional multi-slice 2D spin-echo (SE) sequence where 90° and 180° pulses were calibrated prior to each experiment. Values used for the different experimental parameters will be mentioned later for each specific experiment.

To study fractions of water with restricted mobility (short T2* values), three-dimensional images were acquired using SPRITE (*12*), which is an SPI sequence variant. It is beyond the scope of this work to describe the principles of SPI techniques, which can be found elsewhere (*6*−*13*). For all SPI experiments, pulses of 1.2 $\mu$s (corresponding to a 4.5° flip angle excitation) were used. Polymeric component in the coils caused a background signal in the SPRITE; therefore, the field-of-view (FOV) had to be chosen large enough to avoid folding of these signals in the images of the system of interest. Receiver filter bandwidth was set to 256 kHz, and no oversampling or signal averaging was used. Other experimental parameters will be provided in detail with each particular experiment.

Images were reconstructed from acquired free-induction-decay (FID) files, using self-developed IDL routines (Interactive Data Language, Research Systems Inc., CO). Further image management and analysis was performed using the software ImageJ (W. Rasband, NIH, Bethesda, MD).


**Figure 1.** (**a**) Two-dimensional MRI section of the system used to test protocol 1. Two sausages and a cheesy cream are wrapped in a soft bread layer. (**b**) Photographs from two different views, showing a pair of sandwiches (control and treated) used to test protocol 2. (**c**) Schematic representation showing the positioning of the package containing the sandwiches.

**Samples.** Two different kinds of multicomponent food systems (snacks) have been studied in this work: a first one, with a low contrast in water activity where moisture transport is expected to be slow (days), and a second one, where high water activity contrast results in fast transport (hours).

The first system (snack) consisted of a thin layer of soft and relatively moist bread, filled with two small sausages and creamy cheese (**Figure 1a**). Water activities of these components were all relatively close to 0.85. Samples were prepared at the Unilever Food and Health Research Institute (Vlaardingen) and sent to the MRI facility (Utrecht) in sealed plastic packages under $N_2$ atmosphere. The systems were delivered at the same day of their preparation. One set of samples was transported in an isolating, cooled (∼5 °C) container, and samples were stored in a refrigerator between scanning sessions. A second set was transported and stored at room temperature (∼20 °C). During MRI scans, temperature was maintained at 7 ± 2 °C and 20 ± 2 °C, respectively, using a flow of cooled air through the magnet bore.

The second set of samples consisted of pairs of sandwiches (**Figure 1b**), each one prepared using two slices of bread, a block of mozzarella cheese, a slice of cured ham, a slice of tomato, and a leaf of lettuce. No attempt was made to match the high water activities of the cheese, ham, tomato, and lettuce to the relative low water activity of the bread. The bread used for both sandwiches originated from the same baked piece, and all components used in any of the sandwich pairs had exactly the same mass. In one of the sandwiches, a thick layer of pesto acted as a barrier between the bread and the wet components, the other one acted as a reference. To ensure a correct time frame for the experiments, sandwiches were delivered within 2 h after their preparation. Samples were transported in isolating, cooled (∼5 °C) containers, and the scanning process began immediately upon the arrival of the samples to the MRI facilities. During MRI scans, temperature was maintained at 7 ± 2 °C, using a cooled air flow through the magnet bore. The pairs of sandwiches were placed in a special designed plastic container in order to be located in the magnet bore at ca. 60° angle with the vertical axis (**Figure 1c**), reflecting the condition during (intended) shelf life and display of these products.

**Protocol 1.** The wide range of molecular mobilities (T2 and T2* values) of the protons present in a multicomponent food products (from tens of microseconds to tens of milliseconds) hampers their complete coverage with a single set of experiments. For that reason, protocol 1 comprises 5 different sets of experiments. SET01/02/03 are SPRITE experiments that sample T2* in the microsecond to millisecond range. SET04/05 are spin−echo experiments that sample T2 above the millisecond range.

*SET 01:* 8 SPRITE images; phase encoding times ($t_p$) ranging from 40 to 75 $\mu$s in steps of 5 $\mu$s; TR = 0.75 ms; 50 ms delay between SPRITE ramps; FOV = 7 × 7 × 8 cm$^3$; matrix = 40 × 40 × 32 points (giving a spatial resolution of 1.75 × 1.75 × 2.5 mm$^3$); acquisition time ∼ 15 min (8 × 1 min 42 s). T2* and proton density (M0) maps for this range of mobilities were constructed from these images using a monoexponential decay model of the type $S = C + M0 \exp(-TE/T2)$. Here $S$ is the signal intensity, TE is the encoding time ($t_p$) used for image acquisition, T2 is the transverse relaxation time (T2* in SPI techniques), and $C$ is a constant that includes the signal contribution from nonrelaxed (long T2/T2* values) components.

*SET 02*: 8 SPRITE images; $t_p$ ranging from 100 to 450 $\mu$s in steps of 50 $\mu$s; TR = 1.5 ms; 50 ms delay between SPRITE ramps; FOV = 7 × 7 × 8 cm$^3$; matrix = 64 × 64 × 32 points (giving a spatial resolution of 1.1 × 1.1 × 2.5 mm$^3$); acquisition time ~ 40 min (8 × 5 min). T2* and proton density (M0) maps were constructed from these images with the same monoexponential decay model used for SET 01.

*SET 03*: 35 SPRITE images; $t_p$ ranging from 0.5 to 3.9 ms in steps of 100 $\mu$s; TR = 4.5 ms; no delay between SPRITE ramps; FOV = 7 × 7 × 8 cm$^3$; matrix = 64 × 64 × 32 points (giving a spatial resolution of 1.1 × 1.1 × 2.5 mm$^3$); acquisition time ~ 5 h 45min (35 × 9 min 50 s). Similar to gradient-echo pulse sequences, SPI sequences use only an excitation radio frequent (RF) pulse (no refocusing pulse), and therefore, in a specific regime of molecular mobilities (from 0.7 ms at 4.7 T), two different out-of-phase signals produced by water and fat protons, respectively, are observed (*14*). For this reason, in this set of experiments, T2* and proton density maps for water and fat molecules were constructed by fitting the acquired images to the following equation:

$$S = C + (\mathrm{M0w}\cdot e^{(-\mathrm{TE}/\mathrm{T2*_w})}) + (\mathrm{M0f}\cdot e^{(-\mathrm{TE}/\mathrm{T2*_f})}\cdot \sin(a + b\cdot \mathrm{TE})) \quad (1)$$

where M0w and M0f correspond to water and fat proton densities, respectively, $T2*_w$ and $T2*_f$ correspond to water and fat spin−spin relaxation times, and $a$ and $b$ are constants that characterize the dephasing of water and fat spins. $C$ is a constant accounting for signal contribution of slowly decaying proton signals (long T2 values). Since seven fitting parameters have to be optimized, 35 instead of 8 images with different encoding times were acquired.

*SET 04*: 8 SE images; echo times (TE) = 5.6, 7.7, 11, 15, 21, 29, 40, and 50 ms; TR = 3 s; FOV = 6.4 × 6.4 cm$^2$; matrix = 64 × 64 points (giving a spatial resolution of 1.0 × 1.0 mm$^2$); 2 slices of 2 mm; 2 averages; acquisition time ~ 50 min (8 × 6.5 min). T2 and proton density (M0) maps were constructed from these images using a monoexponential decay model.

*SET 05*: 8 SE images; TE = 50, 58, 68, 80, 94, 110, 130, and 150 ms; TR = 3 s; FOV = 6.4 × 6.4 cm$^2$; matrix = 64 × 64 points (giving a spatial resolution of 1.0 × 1.0 mm$^2$); 2 slices of 2 mm; 2 averages; acquisition time ~ 50 min (8 × 6 min 25 s). T2 and proton density (M0) maps were constructed as above.

The resulting total scanning time (8 h 20 min) was quite long, mainly for two reasons: (1) the use of (time-consuming) SPI sequences to assess short T2* fractions and (2) the need for the acquisition of a large number of images in SET 03 to accurately fit the data to the needed multiexponential model proposed. Hence, time resolution of this protocol is only suitable to follow slow moisture transport processes (days). In return, it provides detailed information of all mobility fractions present in the system.

**Protocol 2.** This protocol was designed to follow faster moisture transport processes. This improvement of temporal resolution compromises the other three imaging requirements. Since the main cause of the long scanning time required in protocol 1 is the need for a high number of images for the third set of experiments, a reduction in the spatial resolution to half or even to one-fourth would not be enough to reduce scanning time. An additional handicap in our particular study consisted of the fact that the samples we intend to study using this protocol (sandwiches) are larger than those used for protocol 1. Therefore, the time resolution gained by sacrificing spatial resolution would be annulled by the need of a larger scanning matrix. Since maximal sensitivity and visualization of immobilized fractions of water have high priority in our studies, the only thing we can do to increase temporal resolution is to reconsider the range of molecular mobilities to be studied.

Our main goal in this study was to find means to assess moisture transport among different components of multicomponent products in order to design strategies to control moisture transport. For that purpose, it would be sufficient, although not ideal, to acquire a single SPI image using an encoding time as short as possible. If this time is short enough, only protons from the crystalline/glassy components (mainly starch and solid fat) would be relaxed when the image is acquired (no T2* weighting). Any change detected in signal intensity would be directly proportional to changes in proton density of the water and fat molecules present in the sample. Considering the characteristics of the system under study, and the temperature at which sandwiches are stored and measured (7 ± 2 °C), it is expected that moisture transport is the dominant process. Nevertheless, differentiation of signal changes due to water and fat migration is a known limitation of the proposed methodology.

In this protocol, a single SPRITE image was acquired using the following experimental parameters: $t_p$ = 50 $\mu$s; FOV = 9.6 × 9.6 × 12 cm$^3$; matrix = 128 × 128 × 60 points (giving a spatial resolution of 0.75 × 0.75 × 2 mm$^3$); TR = 3 ms; 300 ms delay between SPRITE ramps; scanning time = 1 h 30 min.

A capillary filled with water doped with $MnCl_2$ (with an ultra-short T2* value) was included within the FOV to calibrate the images for absolute moisture content (per volume element). Prior to the time series of experiments, an image of a bottle filled with the same doped solution, but occupying the complete field-of-view, was acquired using the same parameters to correct the images for spatial RF inhomogeneities.

## RESULTS AND DISCUSSION

**Detailed Monitoring of Slow Moisture Migration Processes (Protocol 1).** To assess the feasibility of detailed monitoring of relatively slow migration processes, a system was chosen where the water activities of the different components matched. The system consisted of a bread roll filled with cream cheese and two sausages (**Figure 1a**), and was monitored at two different temperatures (7 and 25 °C) during two weeks.

After acquiring the five designed sets of experiments, the obtained images were used to calculate six different T2* (or T2) and proton density maps. Maps obtained for both samples (studied at 7 and 25 °C, respectively) at day 1 of the study are presented in **Figure 2**. Similar maps (not shown) were obtained for successive days of the study (2, 3, 4, 7, 10, and 15). T2 maps reflect absolute T2 or T2* values calculated using a monoexponential model for sets 01, 02, 04, and 05. For SET03, eq 1 provides two different T2* and proton density maps for water protons and fat protons. In **Figure 2**, M0 maps reflect proton densities expressed as percentage, in a scale in which 100% corresponds to free water (calculated using a $MnCl_2$ doped water solution). In most of the maps, two different regions of interest (ROIs) were identified. A first one, corresponding to the outer bread layer, was visible in all maps except for those obtained using SET05, and a second one corresponding to the filling material (two sausages and a cheese cream, which could not always be distinguished), also visible in all maps.

In **Figure 2**, histograms showing different fractions of water and fat molecules of different mobility obtained from these T2/T2* maps (at 7 °C) are also presented. Similar histograms were constructed for the sample at 25 °C and for different time points showing similar results (data not shown). To be able to present a wide range of T2*/T2 values, these values are presented in logarithmic scale ranging from a T2*/T2 value of 1 $\mu$s to 100 ms. Areas of the different populations of protons have been normalized using the proton densities obtained in the M0 maps (the reader must be careful when visually comparing areas on a logarithmic scale).

Some of the information obtained from the different sets of experiments seems to be redundant (overlapping T2*/T2 distributions), and in general we can establish the existence of three mobility fractions for each component of the system: (1) a fraction of molecules with very low mobility (fraction F1: 10 $\mu$s < T2* < 100 $\mu$s), corresponding to material in a crystalline-glassy state and mainly detected in SET01, (2) a fraction of water with moderate mobility (fraction F2: 100 $\mu$s < T2* < 1 ms), corresponding to mesomorphic states, mainly

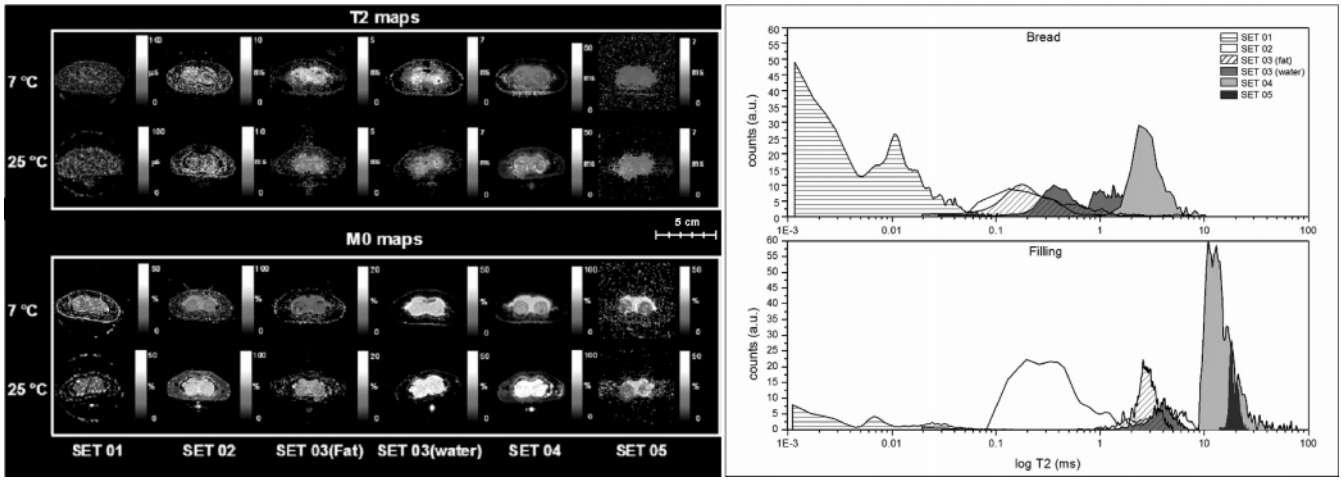


**Figure 2.** (Left) T2 maps and proton density maps (M0) as calculated using the five sets of experiments performed (day 1) using protocol 1 at 7 and 20 °C. From SET 03, two different pair of maps (water and fat) were obtained. For every set a scale was chosen that showed best image contrast. (Right) Histograms (in logarithmic scale) showing T2 populations obtained from those maps in two selected ROIs (bread and filling material).

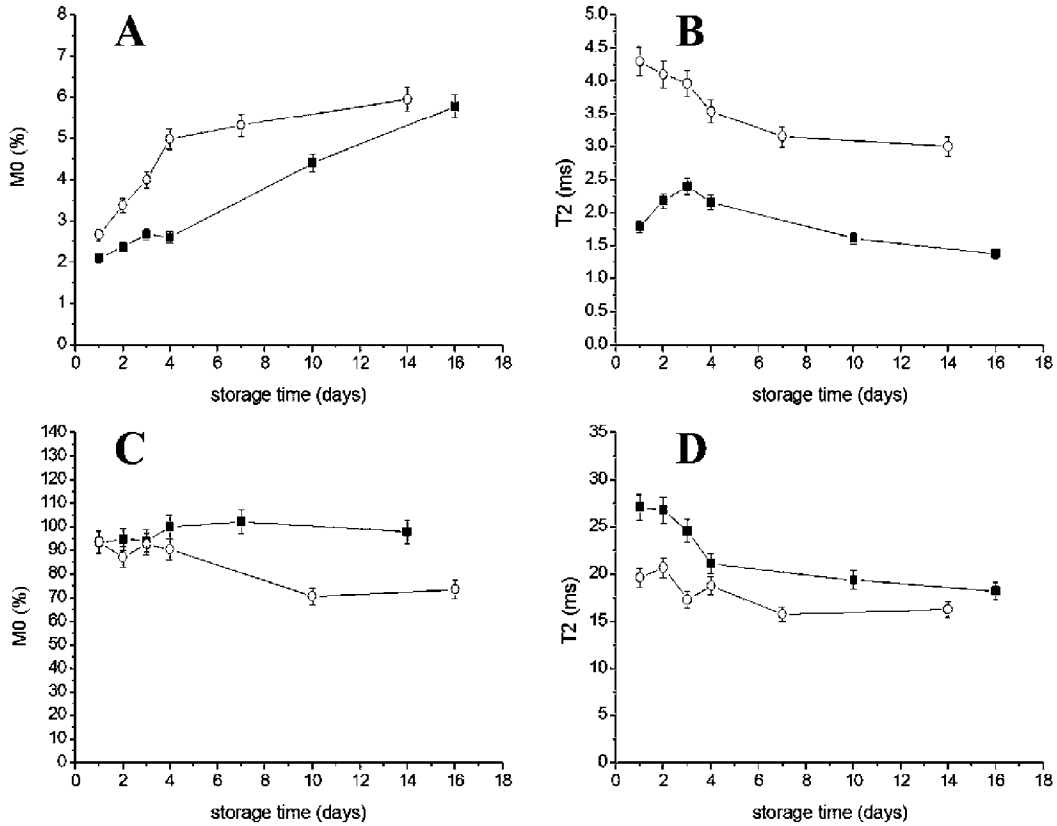


**Figure 3.** Variation of M0 (**A**, **C**) and T2 (**B**, **D**) vs time observed for the fractions of water molecules that changed during storage. Parts **A** and **B** represent the soggy (F2) component of bread, and parts **C** and **D** correspond to the liquid (F3) component of cheese. Open and closed symbols represent data collected at 25 and 7 °C, respectively. Lines are only drawn for visual orientation. Experimental errors are indicated by bars and are typically in the order of 5%.

detected in SET02 and SET03, and (3) a fraction of mobile water molecules (fraction F3: T2 > 1 ms), mainly detected in SET03, SET04, and SET05. We have to keep in mind the limitations of the fitting of the SET01 data, since the lowest encoding time we could use in our system was 40 $\mu$s. For the bread, 71% of the protons had a low (F1 22%) or intermediate (F2 49%) mobility. As a consequence, they are very difficult to detect using conventional MRI techniques (bread is not visible in SET05 and barely visible in SET04). For the filling materials (sausage and cheese), most of the protons (60%) had moderate to high mobility (F3).

Mean T2/T2* and M0 values of both ROIs (bread and filling material) of the low, intermediate, and high mobility fractions were analyzed as a function of the storage period of the products. Due to the relative small differences in water activity in our system, only two of the different water fractions present in the system experienced main changes during the studied period (**Figure 3**). During storage one can observe migration of water from the liquid (F3) cheese component (**Figure 3C**) to the intermediate (F2) mobility component of the bread (**Figure 3A**). We note that since the bread (F2) and cheese (F3) represent a selection of the protons present in the system, the graphs in

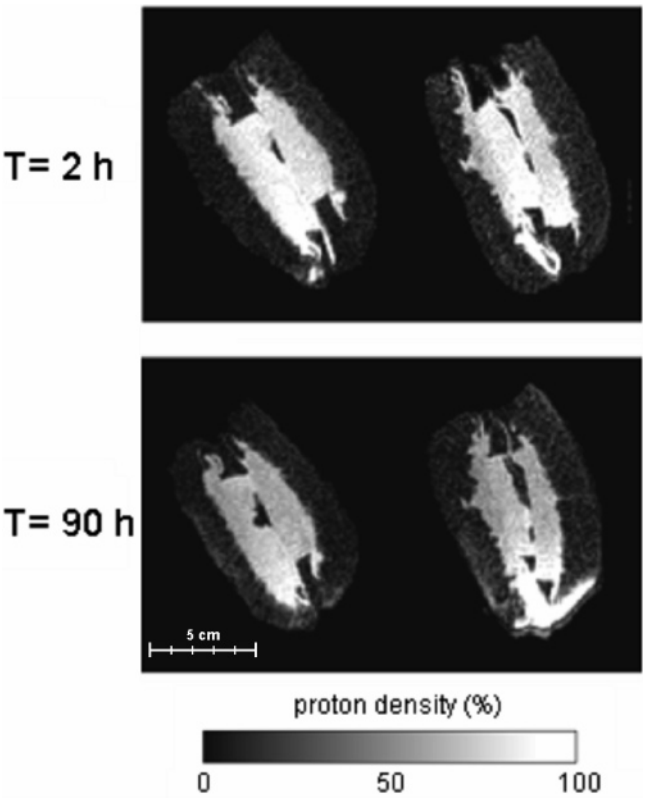


**Figure 4.** Two-dimensional slices obtained from the acquired 3D-MRI images, depicting proton densities for a sandwich at two different time points: 2 h (left column) and 90 h (right column) after preparation of the sandwiches. The left sandwich is the treated, and the right sandwich is the untreated (control) one. In the scale of proton densities, 100% corresponds to the signal of free water.

**Figure 3A,C** cannot be used for mass balancing. These graphs do show that the kinetics of moisture migration is faster at 25 than at 7 °C. As a result of moisture migration one can also observe that both the T2* values of the soggy bread (**Figure 3B**) as well as the T2 of the mobile cheese component (**Figure 3D**) show a decrease. Whereas the decrease of mobility for the mobile cheese component can be explained from dehydration, this is less trivial for the bread component. Currently, we attribute the decrease in molecular mobility in the F2 bread component during storage by retrogradation of the starch, concomitant to the ingress of moisture.

In summary, during storage moisture migrates from mobile cheese to the immobile bread component. This results in sogginess of the bread and dehydration of the cheese, thus deteriorating the quality of the product. The sausages show virtually no change during the studied period. Changes at 25 °C happened faster but were similar to those at 7 °C.

**Monitoring of Rapid Moisture Migration Processes (Protocol 2).** To assess the ability of protocol 2 to detect and quantify the relative rapid transport in systems with large differences in water activity, a pair (**Figure 1b**) of treated−untreated model sandwiches was studied. In the left sandwich a moisture barrier was applied in the form of a thick pesto layer. This model system was monitored during a period of 96 h after their preparation, obtaining in total 46 3D-MR images (one every 2 h). From each 3D set of images acquired, 2D sections of the sandwiches were analyzed (**Figure 4**). Since different 2D slices along the long axis of the sandwich showed comparable results, only a central section of the 3D images is presented in this work.

In **Figure 4**, the central 2D sections of the sandwich pair are presented for an early (∼2 h) and a late (90 h) time period of the study. Absolute moisture concentrations in different regions of interest in the sandwiches can be obtained by calibrating the images using an image from a $MnCl_2$ doped water solution, acquired by using exactly the same MR parameters. Thus, in a scale where 100% corresponds to the signal produced by free water, moisture concentrations (MC) obtained at time $t = \sim 2$ h were as follows: tomato = 77 ± 4%, cheese = 67 ± 5%, ham = 67 ± 3%, and bread ranged between 8 and 10 ± 1%, depending on position in the sandwich. When one takes into account that these concentrations are expressed per volume element, we observe that these values are in rough agreement with reported values (*15*). We note that the achieved spatial resolution did not allow us to estimate changes in water concentration of the lettuce in any of the sandwiches.

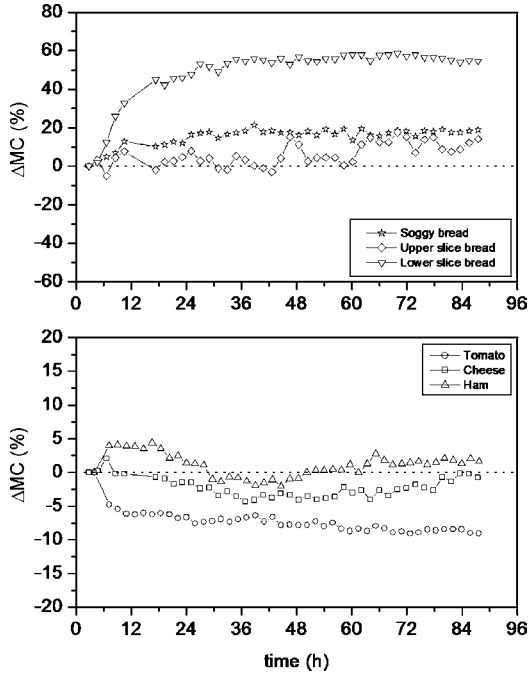


**Figure 5.** Variation of moisture content (ΔMC) from the untreated sandwich with respect to the treated one, expressed as percentage of change versus time for different components identified on the sandwich (as indicated in the plot inserts).

In the images in **Figure 4**, a high proton density (high amount of moisture) is visible at the bottom of the untreated sandwiches at time $t = 90$ h. This is the result of moisture migration, due to joint action of Aw differences and gravity. From the differences between the treated and untreated sandwich one can already qualitatively conclude that the pesto moisture barrier was effective. A more quantitative approach is presented in **Figure 5**, where the migration processes is quantified by selecting different ROIs in the images and plotting the mean value of the signal intensity versus time. Here the difference in signal intensity of the same ROIs selected in both the treated and untreated sandwich (ΔMC) is plotted versus time. Note that these regions represent a selection of the system and no mass balance can be derived from them. Mass balance has been verified by integrating over the complete system, and this indeed demonstrated that signal intensity was conserved during storage time.

The curves in **Figure 5** show that, in the untreated sandwich, the tomato lost significantly more moisture than the treated one. The other two moist elements (cheese and ham) showed a minor loss of moisture, identifying the tomato as the major source. In all selected regions of the bread, a higher uptake of moisture was detected for the untreated sandwich, especially for the lower

slice of bread. This illustrates that, in the untreated sandwich, part of the moisture transport is gravity driven, leading to bread sogginess in the lower part. In the treated sandwich all results point toward less moisture migration, and this convincingly demonstrates the effectiveness of the pesto layer as a moisture barrier.

Although the use of MRI for studying solidlike materials remains a challenge, we have successfully shown how moisture (re)distribution among components with a broad range of molecular mobility regimes can be monitored in a quantitative manner. Two protocols have been defined that emphasize different features of the MRI experiment: resolution of different mobility regimes vs time resolution. In the first proposed protocol, temporal resolution was not emphasized and long scanning times enabled the monitoring of changes in moisture content and mobility for all fractions of water molecules present in the system for long storage periods. In our second protocol, the increased temporal resolution was adequate to follow the kinetics of moisture migration on a time scale of hours, at the expense of resolving components with different molecular mobility.

With the proposed MRI protocols we have established a tool to quantify dynamic changes noninvasively, thus enabling the rational design of strategies to diminish or retard the inevitable moisture (re)distribution process during shelf life. The MRI measurements can also be deployed to define and validate models to describe, and ultimately predict, moisture transport processes. The development and validation of such models (*4*, *5*) was out of the scope of this work and will be pursued in a future study.

## ABBREVIATIONS USED

FOV, field of view; MRI, magnetic resonance imaging; M0, magnetization density; RF, radio frequent; ROI, region of interest; SE, spin−echo; SPI, single point imaging; SPRITE, single point ramped imaging with T1 enhancement; TE, echo time; $t_p$, dephasing time; TR, relaxation recovery time.

## LITERATURE CITED

(1) Labuza, T. P.; Hyman, C. R. Moisture migration and control in multidomain foods. *Trends Food Sci. Technol.* **1998**, *9*, 47−55.

(2) *Water management in the design and distribution of quality food*; Roos, Y. H., Leslie, R. B., Lillford, P. J., Eds.; Technomic Publishing: Lancaster, USA, 1999.

(3) Guillard, N.; Broyart, B.; Guilbert, S.; Gontard, N. J. Evolution of moisture distribution during storage in a composite food, modelling and simulation. *Food Sci.* **2003**, *68*, 958−966.

(4) Guillard, N.; Broyart, B.; Guilbert, S.; Gontard, N. Preventing moisture transfer in a composite food using edible films: experimental and mathematical study. *J. Food Sci.* **2003**, *68*, 2267−2277.

(5) Guillard, N.; Broyart, B.; Guilbert, S.; Gontard, N. Modelling of moisture transfer in a composite food: dynamic water properties in an intermediate aw porous product in contact with high aw filling. *TransIChemE* **2003**, *81* (A), 1090−1098.

(6) Jones, C. K.; Xiang, Q. S.; MacKay, A. L. Linear combination of multiecho data: Short T2 component selection. *Magn. Reson. Med.* **2004**, *51* (3), 495−502.

(7) Ruan, R.; Chen, P. L., *Water in Foods and Biological Materials. A Nuclear and Magnetic Resonance Approach*; Technomic Publishing: Lancaster, USA, 1998.

(8) Emid, S.; Creyghton, J. H. N. High-resolution NMR imaging in solids. *Physica B* **1985**, *128B*, 81−83.

(9) Gavira, S.; Cory, D. G. Sensitivity and resolution of constant-time imaging. *J. Magn. Reson. Ser. B* **1994**, *104*, 53−61.

(10) Cornillon, P.; Salim, L. C. Characterization of water mobility and distribution in low- and intermediate-moisture food systems, *Magn. Res. Im.* **2000**, *18* (3), 335−341.

(11) Gruwel, M. L. H.; Latta, P.; Volotovskyy, V.; Tomanek, B. Magnetic Resonance Imaging 0f Seeds by Use of Single Point Acquisition. *J. Agric. Food Chem.* **2004**, *52* (16), 4979−4983.

(12) Balcom, B. J.; MacGregor, R. P.; Beyea, S. D.; Green, D. P.; Armstrong, R. L.; Bremner, T. W. Single-point imaging with T1 enhancement (SPRITE). *J. Magn. Reson. Ser. A* **1996**, *131*, 131−134.

(13) Beyea, SD.; Balcom, B. J.; Prado, P. J.; Cross, A. R.; Kennedy, C. B.; Armstrong, R. L.; Bremner, T. W. Relaxation time mapping of short T2* nuclei with single-point imaging (SPI) methods. *J. Magn. Reson.* **1998**, *135*, 156−164.

(14) *Magnetic Resonance Imaging: physical principles and sequence design*; Haacke, E. M., Brown, R. W., Thompson, M. R., Venkatesan, R., Eds.; Wiley-Liss: New York, NY, 1999.

(15) Gerbhardt, S. E.; Robin, R. G. *Nutritive Value of Foods*; Home and Garden Bulletin 72, U.S. Department of Agriculture, 2002.

**Received for review September 12, 2005. Revised manuscript received November 30, 2005. Accepted December 3, 2005. This work has been supported by the Dutch BTS program (Dutch Ministry of Economical affairs) as project BTS00103.**

JF052246Z